J Electroceram (2008) 21:331–335
DOI 10.1007/s10832-007-9161-z

# Bilayered $Pb(Zr,Ti)O_3/(Bi,Nd)_4Ti_3O_{12}$ thin films

**C. H. Sim · J. M. Xue · X. S. Gao · Z. H. Zhou · J. Wang**

Published online: 1 May 2007
© Springer Science + Business Media, LLC 2007

**Abstract** Bilayered ferroelectric thin films consisting of $Pb(Zr_{0.52}Ti_{0.48})O_3$ (PZT) and $(Bi_{3.15}Nd_{0.85})Ti_3O_{12}$ (BNT) have been successfully synthesized on $Pt/Ti/SiO_2/Si$ substrates, via a combined sol–gel and rf-sputtering route. Their ferroelectric and dielectric properties are critically dependent on the phases present, film texture and in particular layer and film thicknesses. Due to the coupling of PZT and BNT bilayers, there requires an optimized thickness combination of the two ferroelectric layers, in order to give rise to the wanted ferroelectric and dielectric properties, while the phenomenon can not be accounted for by the simple series connection model.

**Keywords** Multilayered thin films · PZT · BNT · Ferroelectric behaviors

## 1 Introduction

Ferroelectric thin films, which are compatible with the existing Si integrated circuit technology, have attracted extensive research for applications in non-volatile, random access memory (FRAM) and microelectromechanical system (MEMS) [1, 2]. A number of studies have been made with the electrical properties of individual $Pb(Zr_{0.52}Ti_{0.48})O_3$ (PZT) and $(Bi_{3.15}Nd_{0.85})Ti_3O_{12}$ (BNT) thin films for these applications [3–6]. PZT possesses attractive ferroelectric and dielectric properties, which make it a promising candidate. However, its polarization fatigue is a principal drawback for applications [3, 4]. On the other hand, BNT is of resistance to polarization fatigue despite its relatively poor ferroelectric and dielectric properties [5, 6]. It is therefore of interest to study the feasibilities of effectively combining PZT and BNT, in order to improve the electrical properties of ferroelectric thin films.

The coupling and interaction among the layers in multilayered/heterolayered structure can significantly improve the functional properties of ferroelectric and piezoelectric thin films. For instance, giant polarization (79 $\mu C/cm^2$) has been achieved in heterolayered films consisting of alternating $Pb(Zr_{0.8}Ti_{0.2})O_3$ and $Pb(Zr_{0.2}Ti_{0.8})O_3$ layers [7]. The much improved ferroelectric properties were accounted for by the coupling of the rhombohedral and tetragonal layers. Similarly, $BiFeO_3/SrRuO_3/SrTiO_3$ also shows enhanced polarization properties by heteroepitaxial stabilization of monoclinic phase in $BiFeO_3$ [8]. In the present study, PZT/BNT bilayered thin films were deposited on $Pt/Ti/SiO_2/Si$ substrates and their electrical properties were investigated. Three combinations containing different PZT to BNT layers of different layer thicknesses were fabricated.

## 2 Experimental details

The substrates used in this study were $Pt/Ti/SiO_2/Si(1\ 0\ 0)$. PZT layers of thickness $d_1$ were first deposited on the substrates followed by the BNT layers of thickness $d_2$. The total thicknesses of the bilayered films ($d_1+d_2$) were controlled at 450 nm with a tolerance of 10%, while the ratio $d_1:d_2$ was varied from 1:2, 1:1 to 2:1. The three bilayered films are coded as 150PZT/300BNT, 225PZT/225BNT and 300PZT/150BNT, respectively, where the thicknesses of corresponding ferroelectric layers are indicated.

C. H. Sim · J. M. Xue · X. S. Gao · Z. H. Zhou · J. Wang (✉)
Department of Materials Science and Engineering,
National University of Singapore,
Science Drive 4,
Singapore 119260, Singapore
e-mail: msewangj@nus.edu.sg

The PZT layers were prepared via a sol–gel route using lead acetate ($Pb(CH_3COO)_2 \cdot 3H_2O$), zirconium isopropoxide ($Zr[OCH(CH_3)_2]_4$) and titanium isopropoxide ($Ti[OCH(CH_3)_2]_4$) as the starting materials. Ethylene monomethyl ether ($CH_3OCH_2CH_2OH$) and acetic acid ($CH_3COOH$) at volume ratio of 3:1 were chosen as the solvent. The concentration of sol solution was controlled at 0.4 M with 5 mol% of excess Pb to compensate for Pb loss at the heat treatment temperature. The sol solution was spin-coated onto the substrate at 3,000 rpm for 30 s. The gel films were dried at 300 °C for 5 min and baked at 500 °C for 20 min before being annealed at 650 °C for 30 min.

The BNT layers were deposited on PZT films by rf-sputtering. The starting materials of the sputtering target were bismuth oxide ($Bi_2O_3$), neodymium oxide ($Nd_2O_3$) and titania ($TiO_2$). Excess Bi of 5 mol% was added to compensate for the likely Bi loss at the annealing temperature. They were mixed by ball-milling and pressed into pellet before being sintered at 1,000 °C for 1 h. Deposition of BNT films were performed at room temperature with a base pressure of $10^{-6}$ Torr, deposition pressure of 20 mTorr and rf power of 100 W. The as-deposited films were then crystallized under 700 °C for 3 min by rapid thermal processing (RTP).

To characterize their electrical properties, Au dots of 0.1 mm radius were deposited on the bilayered films as the top electrode. Single layered BNT and PZT films of comparable thicknesses (coded as 450BNT and 450PZT, respectively) were also synthesized for comparison purposes. Phase evolutions in the bilayered thin films were monitored using an X-ray diffractometer (Bruker D8 Advanced XRD). The texture development was determined by a field emission scanning electron microscope (Phillips XL30 FE-SEM) and a scanning probe microscope (Nanoscope IIIa, Digital Instruments). Ferroelectric analyzer (Radiant Technologies) and impedance analyzer (Solartron SI 1260) were used to investigate the ferroelectric and dielectric behaviors of these films.

## 3 Results and discussions

Phase development of the bilayered thin films was monitored at various stages of film deposition and thermal annealing. X-ray diffraction (XRD) patterns in Fig. 1 clearly show that both BNT and PZT were successfully retained in all the bilayered films. No other unknown phases were observed. Both bilayered and single layered films appeared dense and crack-free, as shown by the surface morphology micrographs of 150PZT/300BNT and 450BNT in Fig. 2(a). The average grain sizes in the bilayered films are greatly reduced as compared to those of the single layered BNT film (Fig. 2(b)). Figure 2(c) shows the cross-section of 150PZT/300BNT bilayered film. PZT and BNT layers appeared to be densely packed and have rather discrete interface, indicating no apparent interaction between the two stacking ferroelectric films.

Studies of polarization–electric field (*P–E*) loops confirmed that the bilayered films behave rather differently from the single layered PZT and BNT films. Figure 3 shows the *P–E* loops of both the bilayered and single layered films measured at 500 kV/cm. The loops of the bilayered films are not properly saturated before break down. Under an electric field of 500 kV/cm, bilayered films 150PZT/300BNT, 225PZT/225BNT and 300PZT/150BNT exhibit a remanent polarization ($P_r$) of 5.9, 6.7 and 10.3 μC/cm$^2$, respectively. They are greatly improved as compared to the heterolayered film Pt/BLT/PZT/BLT/Pt prepared via sol–

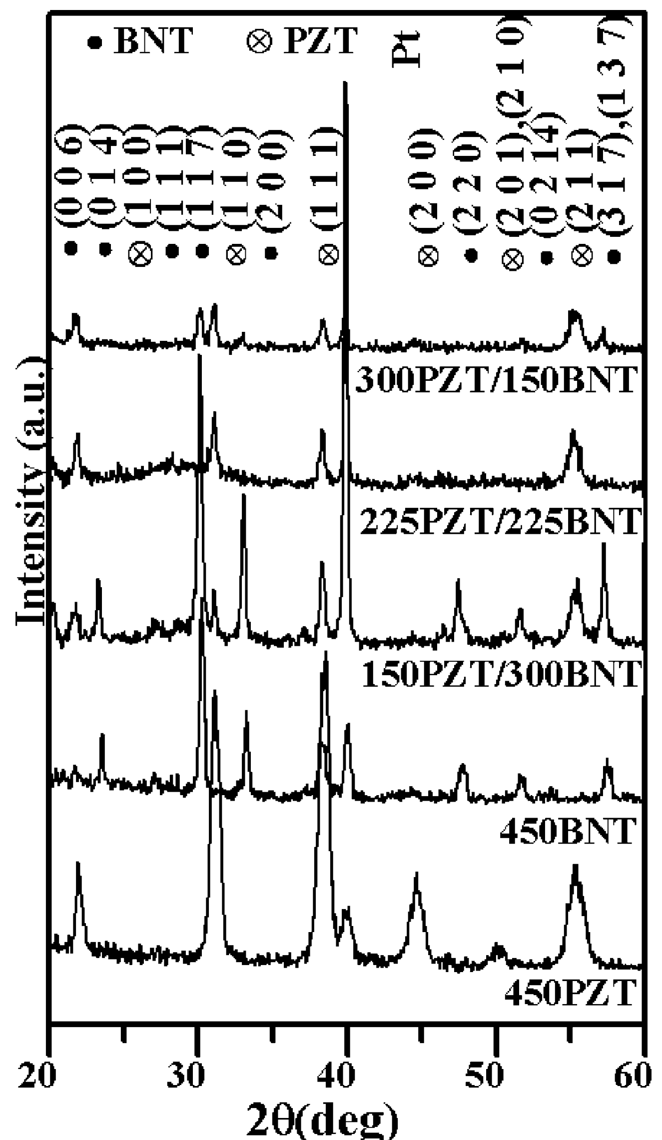


**Fig. 1** XRD pattern of the bilayered and single layered films

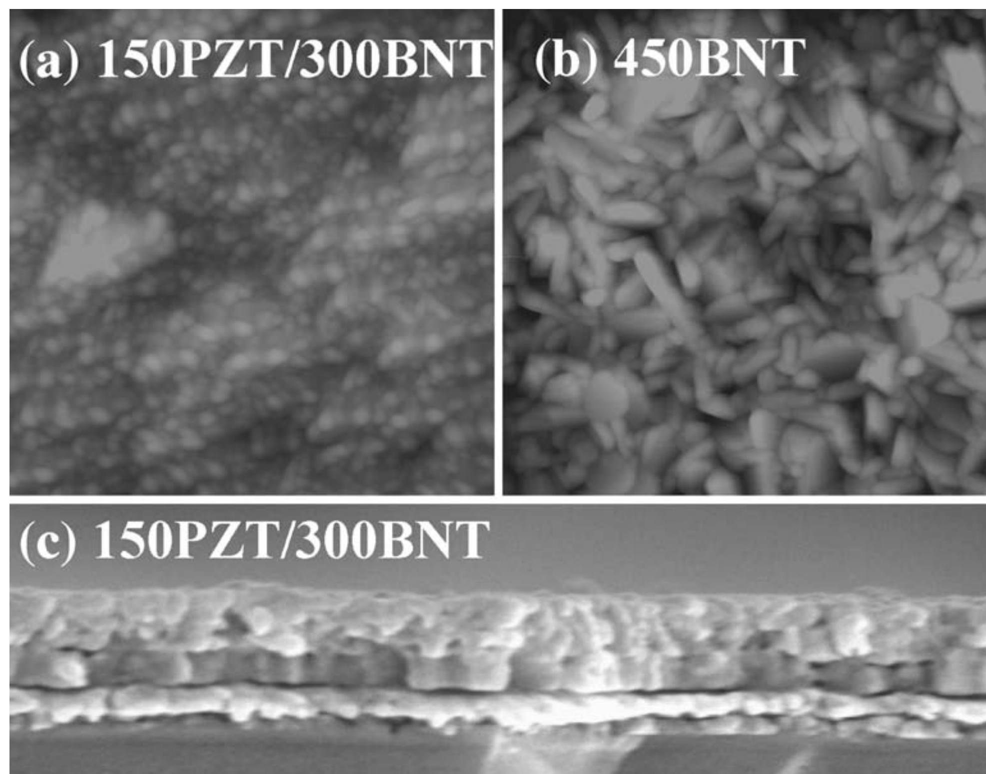


**Fig. 2** (**a**)–(**c**) Micrographs of single layered and bilayered films. (**a**) and (**b**): AFM images of the bilayered 150PZT/300BNT and single layered 450BNT films. (**c**): SEM micrograph of the cross-section of the bilayered 150PZT/300BNT thin film

gel route (4.4 μC/cm$^2$) [9]. As shown in Fig. 4, $P_r$ of the bilayered films is dependent on the thickness of PZT layers in the bilayered films, where it increases with increasing PZT layers thickness. The coercive electric field ($E_c$) at 500 kV/cm is 99.8, 69.2 and 73.6 kV/cm for 150PZT/300BNT, 225PZT/225BNT and 300PZT/150BNT, respectively.

Dielectric behaviors of the bilayered films were determined by applying a small AC current with an amplitude of 0.1 V (root mean squared value). As shown in Fig. 5, the dielectric permittivity ($\varepsilon$) of the bilayered films is dependent on the thickness of BNT layer in the bilayered films, where it decreases with increasing BNT layer thickness, while their dielectric loss (tan $\delta$) are lowered. The improvement in tan $\delta$ suggests that space charge is not the cause for the enhanced permittivity.

To understand the possible couplings between the PZT and BNT layers in the bilayered thin film further, series connection model was considered [10]:

$$\frac{d_t}{\varepsilon_{PZT/BNT}} = \frac{d_{PZT}}{\varepsilon_{PZT}} + \frac{d_{BNT}}{\varepsilon_{BNT}} \quad (1)$$

where $d_t$ and $\varepsilon_{PZT/BNT}$ are the total thickness and of the bilayered films, respectively, $d_{PZT}$ and $d_{BNT}$ are thicknesses

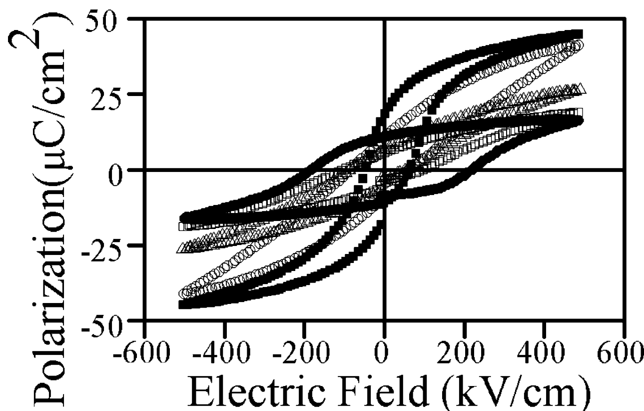


**Fig. 3** *P–E* loops of the bilayered and single layered films at an electric field of 500 kV/cm. *Filled square*: PZT single layered film, *filled circle*: BNT single layered film, *empty square*: 150PZT/300BNT bilayered film, *empty triangle*: 225PZT/225BNT bilayered film, *empty circle*: 300PZT/150BNT bilayered film

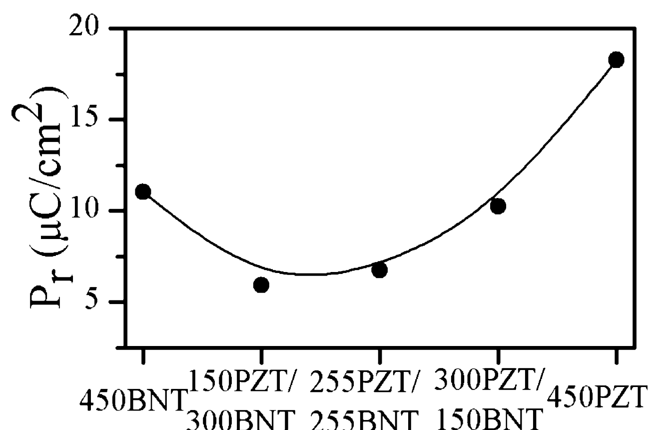


**Fig. 4** $P_r$ of bilayered and single layered thin films at electric field of 500 kV/cm. The *solid line* is guide for the eye to emphasize the $P_r$ change

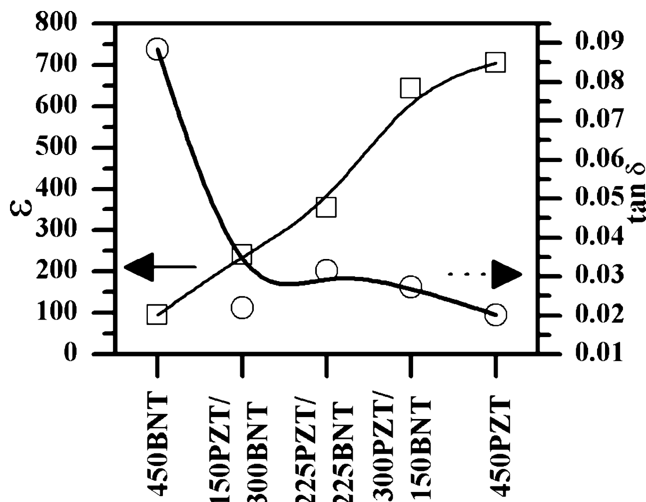


**Fig. 5** Dielectric behaviors of bilayered and single layered films at 10 kHz. The broken lines are guides for the eye to emphasize the dielectric properties change

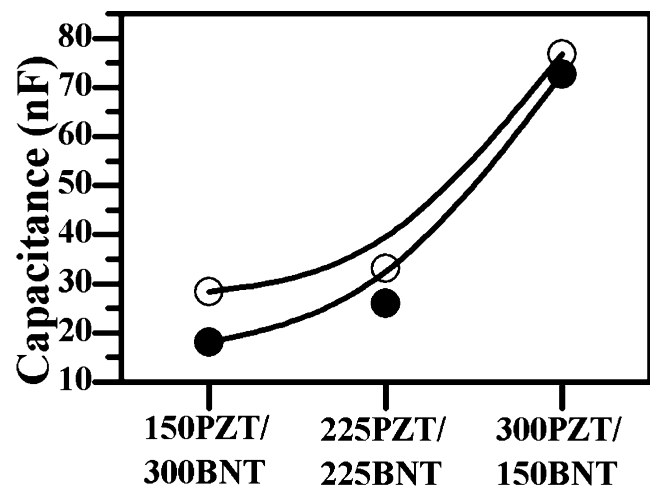


**Fig. 6** Capacitance of bilayered films at 10 kHz. *Empty circle* represents the measured value and *filled circle* represents the calculated value from the series connection model. The *solid lines* are guides for the eye to emphasize the capacitance change

of respective PZT and BNT layers, $\varepsilon_{PZT}$ and $\varepsilon_{BNT}$ are $\varepsilon$ of these respective layers. It is commonly observed that increases with increasing ferroelectric layer thickness [10, 11]. The apparent thickness dependence of $\varepsilon$ is due to the presence of a low-$\varepsilon$ interface layer [11]. To obtain the term on the left hand side of Eq. 1, thickness-independent $\varepsilon_{PZT}$ and $\varepsilon_{BNT}$ on the right hand side are required. Following reference [11], $\varepsilon_{PZT}$ and $\varepsilon_{BNT}$ can be separated from the effect of interface by considering the series connection of ferroelectric film layers and the film/electrode interface as follows:

$$\frac{d_m}{\varepsilon_m} = \frac{d_f}{\varepsilon_f} + \frac{d_i}{\varepsilon_i} \tag{2}$$

where the subscript $m$ denotes the measured value and subscript $f$ and $i$ indicate film and interface, respectively. Single layered PZT as well as BNT films of four different thicknesses were fabricated in order to obtain $d_m$ and $\varepsilon_m$. According to reference [11], $d_i$ is less than 20 nm while the film thickness in this study is much larger, Eq. 2 can therefore be rewritten as:

$$\frac{d_m}{\varepsilon_m} = \frac{1}{\varepsilon_f} d_m + \frac{d_i}{\varepsilon_i} \tag{3}$$

Plotting the term on the left hand side of Eq. 3 against the measured film thickness, thickness-independent $\varepsilon_{PZT}$ and $\varepsilon_{BNT}$ can then be obtained as a gradient of the linear plot. By substituting the obtained $\varepsilon_{PZT}$ and $\varepsilon_{BNT}$ into Eq. 1, the $\varepsilon$ of the three bilayered thin films can be evaluated.

The capacitances of the bilayered thin film calculated from Eq. 1, as compared to the measured values using impedance analyzer are shown in Fig. 6. Apparently, the calculated capacitances are generally higher than those of measured values. This suggests that a low $\varepsilon$ layer similar to the film/electrode interface in reference [10] can exist in the bilayered films. The dielectric layer could be related to the degradation of ferroelectric properties observed above, where domain locking or screening takes place under an applied electric field as perceived in the bulk ferroelectric film [9, 11]. The exact identity and location of the dielectric layer indeed require further investigation.

Fatigue endurance is one of the main concerns for a ferroelectric thin film. Electric field switching reversal at 300 kV/cm and 200 kHz, the $P_{switch}$—$P_{non\text{-}switch}$ (~$2P_r$) of 300PZT/150BNT shows an increase from 7.54 to 32.97 μC/cm$^2$ before it fell after $10^9$ cycles. A similar increase in $P_r$ was observed in other two bilayered films. For example, such unique phenomenon was reported in reference [12], where it was believed to be related to the breakdown of the dielectric layer present in the bilayered film.

## 4 Conclusion

PZT/BNT bilayered thin films have been fabricated successfully via a combined route of sol–gel and rf-sputtering. A discrete interface between the PZT and BNT layers was observed. XRD patterns showed that PZT and BNT were well preserved, confirming the retention of the two ferroelectric layers. Ferroelectric and dielectric properties of the bilayered films are largely dependent on the layer thicknesses of PZT and BNT layers. Studies using the series connection model suggest the presence of a low- $\varepsilon$ layer in series with the bilayers, which degrades the electrical properties of the bilayered films.

**Acknowledgment** This paper is based upon work supported by the Science and Engineering Research Council—A*Star, Singapore, under Grant No. 022 107 007. The authors also acknowledge the support of the National University of Singapore.

## References

1. J.F. Scott, C.A. Araujo, Science **246**, 1400 (1989)
2. A. Kingon, Nature **401**, 658 (1999)
3. D. Damjanovic, Rep. Prog. Phys. **61**, 1267 (1998)
4. A.K. Tagantsev, I. Stolichnov, E.L. Colla, N. Setter, J. Appl. Phys. **90**(3), 1387 (2001)
5. D. Wu, A. Li, N. Ming, J. Appl. Phys. **95**(8), 4275 (2004)
6. J.H. Li, Y. Qiao, X.L. Liu, C.J. Nie, C.J. Lu, Z.X. Xu, S.M. Wang, N.X. Zhang, D. Xie, H.C. Yu, J.Q. Li, Appl. Phys. Lett. **85**(15), 3193 (2004)
7. Z.H. Zhou, J.M. Xue, H. Zhu, J.M. Miao, J. Appl. Phys. **96**(10), 5706 (2004)
8. J. Wang, J.B. Neaton, H. Zheng, V. Nagarajan, S.B. Ogale, B. Liu, D. Viehland, V. Vaithyanathan, D.G. Schlom, U.V. Waghmare, N. A. Spaldin, K.M. Rabe, M. Wuttig, R. Ramesh, Science **299**, 1719 (2003)
9. D. Bao, N. Wakiya, K. Shinozaki, N. Mizutani, J. Phys. D: Appl. Phys. **35**, L1 (2002)
10. K. Amanuma, T. Mori, T. Hase, T. Sakuma, A. Ochi, Y. Miyasaka, Jpn. J. Appl. Phys. **32**(9B), 4150 (1993)
11. J.J. Lee, C.L. Thio, S.B. Desu, J. Appl. Phys. **78**(8), 5073 (1995)
12. X. Du, I.W. Chen, J. Appl. Phys. **83**(12), 7789 (1998)